

Utility of natural generalised inverse technique in the interpretation of dyke structures

M.M.Malleswara Rao^{1*}, T.V.Ramana Murthy¹, P.Rama Rao², S.Lakshminarayana¹,
A.S. Subrahmanyam¹ & K.S.R.Murthy¹

¹National Institute of Oceanography, Regional Centre, Visakhapatnam-530 017, India

²Geophysics Department, Andhra University, Visakhapatnam – 530 003, India

[*E-mail: mmmrao@darya.nio.org]

Received 15 March 2004, revised 19 May 2005

Forward and Inverse methods of magnetic interpretation have been used to estimate the parameters of dyke like intrusion over the eastern continental shelf of India. In the forward problem, the tentative parameters of the causative source are assumed and anomalies are calculated using the anomaly equation, while inverse problem refers to methods of tracing the boundaries or outlines of anomalous bodies using an iterative approach. While solving the inverse problem, data kernel has been generated through the model (i.e. partial derivatives of magnetic anomaly function with respect to model parameters at each station forming the kernel). In solving the coupled eigenvalue problem of covariance matrices of data kernel, Singular Value Decomposition (SVD) has been performed to build Generalised Inverse Operator (GIO). This GIO is operated on the observed anomaly (with reference to the calculated) to yield improved model parameters. Data and model resolution matrices are computed to check the correctness of the solution and further analysis. The marine magnetic total field anomaly of continental shelf of Visakhapatnam is interpreted using GI technique, which revealed the causative source of the anomaly as a dyke model at a depth of 120 m below seabed.

[**Key words:** Magnetic anomaly, forward problem, inverse problems, GIO, SVD, data resolution, model resolution, closeness ratio, dyke intrusive, Visakhapatnam.]

Introduction

Among the many geophysical techniques, magnetic method is easy to execute and economically viable and therefore widely used in geophysical exploration. A general procedure is to assume most plausible shape for the magnetic anomaly source and compute its magnetic effect at the surface and to modify the model progressively until a reasonable fit with the observed anomaly is obtained¹⁻³. The refined model represents a possible solution. The process of making inferences about the causative source from observed data is what is widely known as the inverse problem. Backus & Gilbert⁴ made an attempt for exploring the mathematical structure of the inverse problems.

The marine magnetic data that were collected in the Bay of Bengal, are interpreted in terms of the geological structures, causing the magnetic anomalies^{5,6}. In the present work, marine magnetic total field anomalies off Visakhapatnam, east coast of India (Fig. 1) inverted by the generalised inverse approach, to yield the intrusive dyke model parameters.

Ultimately the above physical problem gives a mathematical relationship between the theoretical

framework (M : kernel) to observed data (dr) and leading to system of equations (i.e., $M dy = dr$) for solving parameters ($dy = M_g^{-1} dr$, where M_g^{-1} is Generalised Inverse Operator (GIO)). In general the exploration problems are two types: 1) over-determined and 2) under-determined. The trivial solution of even-determined case is of rare

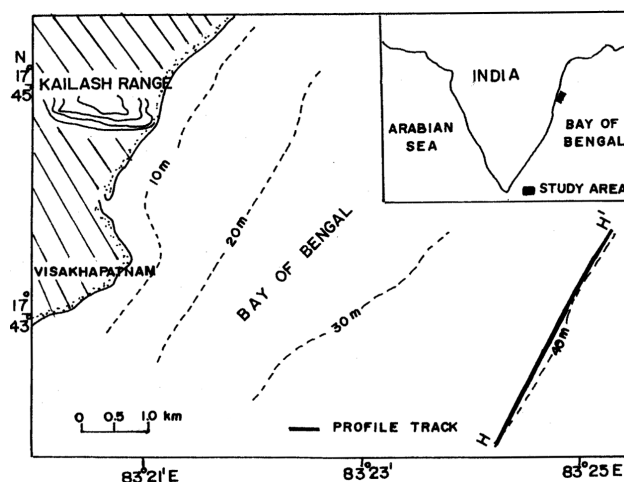


Fig. 1—Parameters of dyke model.

occurrence. In all the cases a good resolution of both the model and data are desirable. The least square method solves the over-determined problem minimizing the squared Euclidean length of the error and has a perfect model resolution. Instead, the under-determined problem can be solved with a perfect data resolution by minimizing the model length. In nature, the problems are neither purely over-determined nor purely under-determined, they are mixed type. The entire field or observation over which the determination of the parameters of the model is to be carried out comes up in observation blocks, some of which are over-determined while some are under-determined leading to non-uniqueness of the solution. The generalized inverse technique solves such a mixed determined problem over the whole region of observations and has both data and model resolutions intermediate between the two extremes⁷. Generalised Inverse (GI) technique through Singular Value Decomposition (SVD) is employed to solve such a mixed determined problem⁷. The advantages of involving SVD in construction of the GIO are viz., (1) SVD is objective and does not impose a pre-determined form to the data; (2) It provides an objective means of ranking uncorrelated modes of variability to determine weak signals or noise from the data; and (3) it provides the modes of variability which are not correlated with one another^{7,8}.

Earlier, Malleswara Rao *et al.*¹, suggested interpretation of magnetic anomalies due to bodies of polygonal cross section using Marquardt⁹ optimisation technique. In the present study, magnetic anomalies due to intrusive dyke model are analysed using the approach of Natural Generalised Inverse (GI) technique¹⁰ as it throws light on data and model resolution and individual model parameter contribution. All these procedures and algorithms attempt to relate physical models to readily observable data and determine the "best-estimates" of model parameters.

Magnetic dyke - forward problem

Dykes and thin sheets are frequently used geophysical models in magnetic studies Radhakrishna Murthy¹¹⁻¹³. The dyke is assumed to be a model with a horizontal top bounded by parallel sides (Fig. 2). Equation for its magnetic anomaly can be written by treating it as a model bounded by four first order surfaces. The conventional method is to write down the magnetic anomaly of a line dipole of cross-sectional area $du . dv$ and integrating it throughout the cross-section of the dyke. When the origin is placed

above the center of the dyke the generalized equation for its magnetic anomaly in any component can be written as (Radhakrishna Murthy¹²):

$$\Delta T(x) = 2J' \int_{z_1}^{z_2} \int_{-w+(v-z_1)\cot\theta}^{w+(v-z_1)\cot\theta} \frac{(v^2 - (x-u)^2) \sin \phi' - 2(x-u)v \cos \phi' dvdu}{((x-u)^2 + v^2)^2} \dots (1)$$

where w is the half-width of the dyke, θ is its dip, z_1 and z_2 are the depths to its top and bottom and

$$J' = J (1 - \cos^2 \alpha \cos^2 D_m)^{1/2},$$

$$\phi' = \phi - \arctan (\sin \alpha \cot D_m)$$

with J , ϕ , α and D_m as defined in notation. The usefulness of the above equation is that one can use the same for calculating vertical, horizontal or total field anomalies by suitably taking the values of D_m . Equation 1 after integration simplifies to

$$\Delta T(x) = 2 J' \sin \theta [\cos Q \cdot (\theta_A - \theta_B + \theta_C - \theta_D) + \sin Q \ln (r_B r_D / r_A r_C)] \dots (2)$$

where various parameters are defined in Fig.2. For special case when the dyke is extending to a large depth $\theta_C = \theta_D$ and $r_D = r_C$. Thus, Eq.(2) takes the form (Radhakrishna Murthy³):

$$\Delta T(x) = C [\cos Q (\theta_A - \theta_B) + \sin Q \ln (r_B / r_A)] \dots (3)$$

The distances and angles involved in Eq. (3) are defined as follows.

$$\theta_A - \theta_B = \arctan ((x+w)/z) - \arctan ((x-w)/z), \text{ for } z \neq 0, \\ r_A^2 = (x+w)^2 + z^2; r_B^2 = (x-w)^2 + z^2 \\ \text{with } Q = \theta - \phi \text{ and } C = 2 J' \sin \theta.$$

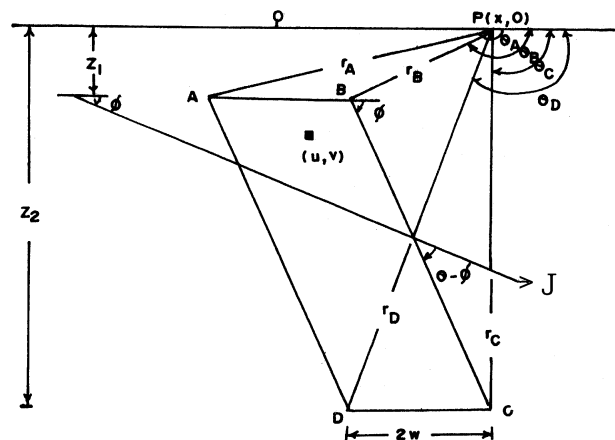


Fig. 2—Magnetic Profile off Visakhapatnam (at 40m depth).

The inverse problem

The generalised equation for the magnetic anomaly of a dyke model is of infinite depth extent shown in Eq:(3). The parameters to be determined from its anomalies are w, z, Q (from $\theta - \phi$), $J \sin \theta$ (from $J' \sin \theta$) and D the position of the center of the dyke. For this, the anomalies $\Delta T(x_i)$ are digitized at distances measured from a convenient reference on the profile. When the distances are measured relative to the reference point, the anomaly equation is rewritten as

$$\Delta T(x_i) = C [\cos Q (\theta_A - \theta_B) + \sin Q \ln (r_B / r_A)] + A'x_i + B', \quad \dots (4)$$

where $A'x_i + B'$ is the associated regional anomaly. Initialization of these parameters is achieved by the procedure suggested by Radhakrishna Murthy¹⁴, which considers the dominant maximum and minimum anomalies and their corresponding distances from the chosen reference point on the magnetic anomaly profile. To calculate the initial values these characteristic distances and/or anomalies are scaled by the computer from the field profile and their ratios or magnitudes are used to calculate the parameters by properly derived empirical relations. The characteristic distances to be measured are chosen, by trial and error, such that they or their ratios vary significantly with one of the parameters and less significantly with others.

Most often the anomalies ΔT_{cal} computed involving these initial parameters differ from the observed anomalies ΔT_{NOBS} . The difference between observed and calculated anomalies at the i^{th} anomaly point is expressed by the Taylor's expansion in terms of errors in the initial values of the model parameters which can be expressed, in terms of errors dw, dz, dD, dQ, dC , regional gradient (A') and constant (B'), in the parameters as follows:

$$\Delta T(x_i) = \Delta T_{obs}(x_i) - \Delta T_{cal}(x_i) \quad (i=1, \dots, N_{OBS}) \quad \dots (5)$$

$$dT(x_i) = \sum_{k=1}^7 \frac{\partial \Delta T(x_i)}{\partial a_k} da_k,$$

where $da_1 = dw, da_2 = dz, da_3 = dD, da_4 = dQ, da_5 = dC, da_6 = dA',$ and $da_7 = dB'$.

The partial derivatives are calculated through the following equations: (Radhakrishna Murthy¹³):

$$\frac{\partial \Delta T(x_i)}{\partial a_1} = 2C \left[\frac{[(x_i - D)^2 + z^2 + w^2]z \cos Q - (x_i - D)[(x_i - D)^2 + z^2 - w^2] \sin Q}{[(x_i - D + w)^2 + z^2][(x_i - D - w)^2 + z^2]} \right],$$

$$\frac{\partial \Delta T(x_i)}{\partial a_2} = 2Cw \left[\frac{[(x_i - D)^2 + z^2 - w^2] \cos Q + 2z(x_i - D) \sin Q}{[(x_i - D + w)^2 + z^2][(x_i - D - w)^2 + z^2]} \right],$$

$$\frac{\partial \Delta T(x_i)}{\partial a_3} = 2Cw \left[\frac{2z(x_i - D) \cos Q - [(x_i - D)^2 - z^2 - w^2] \sin Q}{[(x_i - D + w)^2 + z^2][(x_i - D - w)^2 + z^2]} \right],$$

$$\frac{\partial \Delta T(x_i)}{\partial a_4} = C \left[\frac{[\arctan((x_i - D - w)/z) - \arctan((x_i - D + w)/z)] \sin Q}{[+0.5 \cos Q \ln \{((x_i - D - w)^2 + z^2) / ((x_i - D + w)^2 + z^2)\}]} \right],$$

$$\frac{\partial \Delta T(x_i)}{\partial a_5} = C \left[\frac{[\arctan((x_i - D + w)/z) - \arctan((x_i - D - w)/z)] \cos Q}{[+0.5 \sin Q \ln \{((x_i - D - w)^2 + z^2) / ((x_i - D + w)^2 + z^2)\}]} \right],$$

$$\frac{\partial \Delta T(x_i)}{\partial a_6} = x_i,$$

and

$$\frac{\partial \Delta T(x_i)}{\partial a_7} = 1.0 \quad \dots (6)$$

The necessary normal equations to be solved for the increments da_k ($k=1, \dots, 7$) are framed involving Eq.(3), the observed data and partial derivatives with respect to model parameters and are given by

$$\sum_{i=1}^{N_{OBS}} \sum_{k=1}^7 \frac{\partial \Delta T(x_i)}{\partial a_j} da_k \frac{\partial \Delta T(x_i)}{\partial a_k} (1 + \delta \lambda) da_k \quad \dots (7)$$

$$= \sum_{i=1}^{N_{OBS}} \frac{\partial \Delta T(x_i)}{\partial a_j} dT(x_i), \quad (j = 1 \dots 7)$$

with N_{OBS} = number of magnetic anomaly points, the constant $\delta = 1$ for $i = j$, and 0 otherwise and λ is

Marquardt⁹ damping factor. The Marquardt damping factor λ is chosen by the relation $\lambda = 0.5 [2^{-n} - 1]$ (Radhakrishna Murthy¹³). The value of λ is initially set to zero by putting $n=1$. Subsequently, it is increased or decreased, each time, by one depending upon the resulting objective function is increased or decreased. The Eq.(7) may be put in the matrix form:

$$M dy = dr \tag{8}$$

The Eq. set (8) (for $i = 1, \dots, N_{OBS}$) is to be solved for the increments to the various parameters. To handle this problem there are different approaches that include - a) ridge regression, frequently called Marquardt⁹ iteration and b) Generalized Inversion (GI) approach. In the present magnetic data inversion, we follow the second method viz. GI, as it has additional advantages over the Marquardt method (as already mentioned in the beginning).

Equation (8) is written in following discrete form for computational convenience:

$$dr = M dy ; dr = (dr_i) ; dy = (dy_k) ; (i = 1, 2, \dots, N_{OBS} ; k = 1, 2, \dots, 7) \tag{9}$$

Equation (9) is solved by generalised inverse^{8,15-17} (GI) through singular value decomposition (SVD) to obtain the following optimised model parameters^{10,18} dy_p as follows:

$$M_{(N_{OBS} \times m)} = U_{(N_{OBS} \times r)} \int_{(r \times r)} V^T_{(r \times m)} \tag{10}$$

The columns of U and V are orthonormal i.e. $U^T U = I_{N_{OBS}}$ and $V^T V = I_m$ with $I_{N_{OBS}}$ and I_m are unit matrices of order $(N_{OBS} \times N_{OBS})$ and $(m \times m)$ respectively and $m =$ number of model parameters.

$$\text{In general, } U U^T \neq I_{N_{OBS}} \text{ and } V V^T \neq I_m ; p \leq r = \min(N_{OBS}, m) \tag{11}$$

where r is the rank of the matrix M (data kernel), p number of factors to be considered and the matrices U and V are the respective coupled Eigen vector matrices for the Eigen value problem defined as:

$$(M M^T) U \equiv I^2 U \tag{12}$$

and

$$(M^T M) V \equiv I^2 V \tag{13}$$

In Eq.(10), \int is diagonal matrix of non-zero singular values ($I_i^2 = \lambda_i^2$) of M arranged in the decreasing order. Once U, \int and V are obtained by solving above

Eigenvalue problem (Eqs.12 and 13) the generalised inverse solution (Jackson¹⁸) is given by

$$dy_p = V V^T dy = M^1_g dr \tag{14}$$

where $M^1_g = V_p \int_p^{-1} U_p^T$ is the natural generalised inverse operator(GIO). Let $s(d) = \{u_1, u_2, \dots, u_n\}$ and $s(m) = \{v_1, v_2, \dots, v_m\}$ be sets of orthogonal vectors (i.e., column vectors of complete data space U and model space V) as detailed below:

$U = \{U_p, U_{r-p}, U_0\}$ is the complete data space where U_p : optimised data space-set of p eigenvectors corresponding to dominant eigenvalues such that $\lambda'_1 > \lambda'_2 > \lambda'_3 > \dots > \lambda'_p \neq 0$.

U_{r-p} : set of $(r-p)$ eigenvectors corresponding to remaining dominant eigenvalues such that $\lambda'_{p+1} > \lambda'_{p+2} > \dots > \lambda'_r \neq 0$ and

U_0 : Null space-having eigenvectors corresponding to $r - \min(N_{OBS} \times m)$ zero eigenvalues.

Similarly it follows in the case of complete model space (i.e. $V = \{V_p, V_{r-p}, V_0\}$) and can also be explained.

If $V V^T$ equals to I_m (i.e. the rank of the matrix $M = m$) then the solution of the Eq. (8) is

$$dy_p = dy = M^1_g dr \tag{15}$$

If $V V^T$ not equals to I_m (for the case of, presence of noise in the model space)

$$dy_p \approx dy = M^1_g dr \tag{16}$$

For better estimates the resolution in the model space $V V^T$ of Eq.(16) has to be improved. This is done judiciously by selecting the $p(\leq r)$ eigenvectors (also called factors or modes) in the activated model space $s(m)$ corresponding to the ranking of the p singular values (λ'_i) of the data kernel (M) in descending order. The noise in the data kernel prevailing in the form of small values increases the ranking of the matrix apart from amplifying the solution. This however does not provide any additional information on the model parameters. So, it can be treated as though the solution to the present problem is obtained through the optimisation.

The above process is continued to obtain optimised model based on the best fit between the observed and calculated anomalies. Once the optimised solution is obtained, it is necessary to assess how best the data determines the model parameters. This is done through model resolution ($V_p V_p^T$) and data resolution ($U_p U_p^T$) matrices.

The following mathematical presentation shows us how the data and model space are interrelated. Pre-multiplying (Eq. 14) by V_P^T on both sides of the equation and by defining the general parameters

$$\alpha = V_P^T dy_P \quad \dots (17)$$

$$\Rightarrow \alpha_j = v_j^T \cdot dy_P$$

and

$$\beta = U_P^T dr_P \quad \dots (18)$$

$$\Rightarrow \beta_j = u_j^T \cdot dr_P$$

it reduces to

$$\alpha = T^{-1} \beta \quad \dots (19)$$

The relation shows how data errors in β component belong to small eigenvalues λ'_i (of diagonal matrix Γ) are strongly amplified giving rise to large errors of α_j and hence those components dy , which contributes to α_j . For the investigation of parameter errors and information content of the data it has become tradition to use the model resolution matrix $R = V V^T$ and information density matrix $S = U U^T$.

From Eq. (17) we see that an investigation of the vector v_j will reveal which parameters of dy are specifically attached to the generalised parameters α_j . From Eq. (18) we see that similar investigation of the vector u_j will reveal which data of dr are particularly contributing to the content of the generalised datum β_j . The components of v_j directly indicate which of the parameters of dy are determined. On other hand the components of u_j indicate where to find those data points that contribute to the determination of these parameters v_j^{10} .

Closeness ratio: The ratio between the sum of the factors considered and that of the data matrix (kernel) is the measure of closeness of the model data

$$\text{Measure of closeness} = \frac{\sum_{i=1}^p \lambda'_i}{\sum_{i=1}^r \lambda'_i} \quad \dots (20)$$

where r is the rank of the data matrix M (Kernel). The first eigen function, u_1 associated with the largest eigenvalues λ'_1 represents the gross features (i.e., $\|u_1^T M\|$) in the data in the least square sense, while the second function u_2 associated with second largest eigenvalue λ'_2 describes the residual mean square data [i.e., $\|u_2^T (M - (u_1 u_1^T M))\|$] in the least square sense and so on. The closeness ratio is expressed in percentage to judge the contribution of different parameters.

Synthetic and field example

The efficacy of the natural Generalised Inverse Operator (GIO) is explained in the above GI approach, two numerical experiments were carried out.

Synthetic data:

A synthetic dyke model with $w=4.0$ km, $z=1.0$ km, $D=10.0$ km, $Q = 90^\circ$ and $J = 100$ nT is considered and the magnetic anomaly using the forward anomaly Eq. (3). The synthetic anomaly so generated is subjected to GI and the derived model anomaly and corresponding model (dotted circles) shown in Fig. 3A, which is well coincided with actual model anomaly. The values obtained for the optimized model are $w=4.0$ km, $z=1.07$ km, $D=10.0$ km, $Q=90^\circ$ and $J=100.6$ nT shows the efficacy of the method. The success of synthetic model inversion with GI prompted to carryout the field data inversion again using GI.

Field data:

Marine magnetic total field data was collected, using Baringer Proton precession magnetometer (model M123) off Lawson's Bay (opposite Kailash Hill) of Visakhapatnam ($17^\circ 42'$ N, $83^\circ 17'$ E) along a coast parallel profile (HH') (Fig. 1) at 40 m water depth, covering a distance of 2.5 km, at one-minute polarisation interval. Figure 3B shows the observed magnetic anomaly along this coast parallel profile HH' of Fig. 1. The observed total field marine magnetic data were corrected using 1985 IGRF coefficients (DGRF¹⁹) and the residual data at 26 points on the profile is considered in the present GI analysis. The residual marine magnetic anomaly ranges between -460 to 170 nT with a low of -460nT at 1.25 km from the reference point, flanked by highs on either side, 60nT(left) and 170 nT (right) (Fig. 3B). This magnetic anomaly is subjected to GI to yield optimized dyke parameters. Figure 3B also shows the calculated anomalies of initial and final dyke model using GI.

Results and Discussion

In the present section, computed results of the field data (Fig. 3B) are discussed. SVD of kernel $M_{(26 \times 7)} = U \sqrt{V^T}$ has been performed on residual magnetic data and shown as observed data in Fig. 3B. The column matrices $U = (u_1, u_2, \dots, u_7)$ and $V = (v_1, v_2, \dots, v_7)$ are orthonormal eigenvectors spanning data space $s(d)$ and model $s(m)$ corresponding to eigenvalues λ'_i of diagonal matrix $\sqrt{\lambda'_i}$ (Table 1) computed by solving

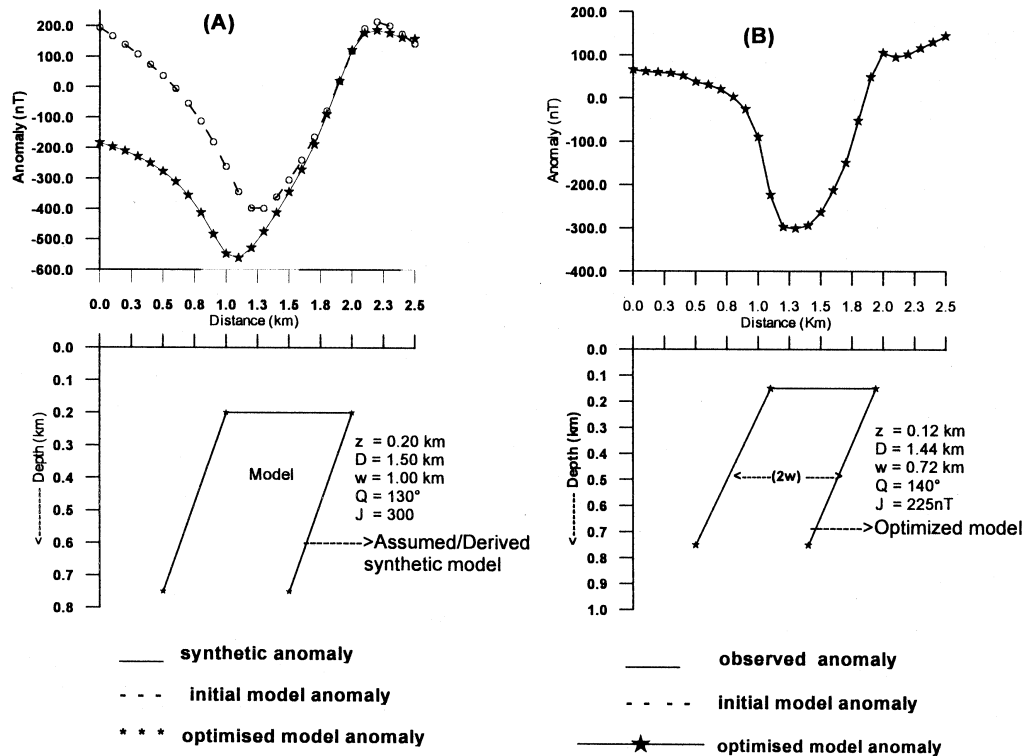


Fig. 3—(A) Synthetic anomaly and its inversion; (B) Field anomaly and its inversion.

Table 1—Eigen values and corresponding closeness ratio for Magnetic dyke model.

Eigen values	Closeness ratio
35.97	58.003
20.36	76.576
17.18	89.804
13.45	97.915
6.60	99.869
1.32	99.946
1.09	100.00

coupled eigen value problem of two covariance matrices MM^T and $M^T M$ of 7 components contributing 100% of total variance. Based on the point of inflection or minimum point of cumulative eigenvalues, four factors ($p=4$) are retained for interpretation as shown in Figs.4 and 5 (however other figures in respect of other 3 factors are also shown for the sake of completeness). The GIO $M_g^I = V_p \sqrt{\lambda_p}^{-1} U_p^T$ has been built after removing null spaces $\{U_0, V_0\}$ to operate on observed magnetic anomaly to yield dyke intrusive model parameters in the present studies (Fig. 3B, field model).

Using vectors in activated space, data resolution matrix $\{U_p U_p^T\}$ and model resolution matrix $\{V_p V_p^T\}$

have been computed and the elements of these matrices are presented in 3-D contour form (Figs.6 and 7) respectively. The diagonal elements of these resolution matrices are presented in Tables 2 and 3. The column Vectors u_i ($i=1, \dots, 7$) of $s(d)$ of corresponding eigenvalues of λ_i (i.e. measure of variance M in descending order), having 26 components and with each component a value that indicates amplitude, which explains sharing contribution of its variance mode i . The component u_i represent the trend or direction of spatial common features contained in kernel M (partial derivatives of magnetic function with respect to model parameters). Its corresponding eigenvalue λ_i represents energy level. In a similar manner, the components of vectors in model space $s(m)$ can be explained. The percentage contribution of individual components of $s(m)$ and $s(d)$ have been computed through closeness ratio approach (Eq. 20) and are shown in Tables 4 and 5. Eigenvectors derived from the data kernel of present field example have been presented in Figs. 4 and 5 to explore the spatial and model parameter variability. From these Figs. 4 and 5 and Tables 4 and 5 the first four eigenfunctions of $s(d)$ and $s(m)$ account for more than 98% of variance relatively dominated by the first function alone. The first function u_1 and v_1 contribute

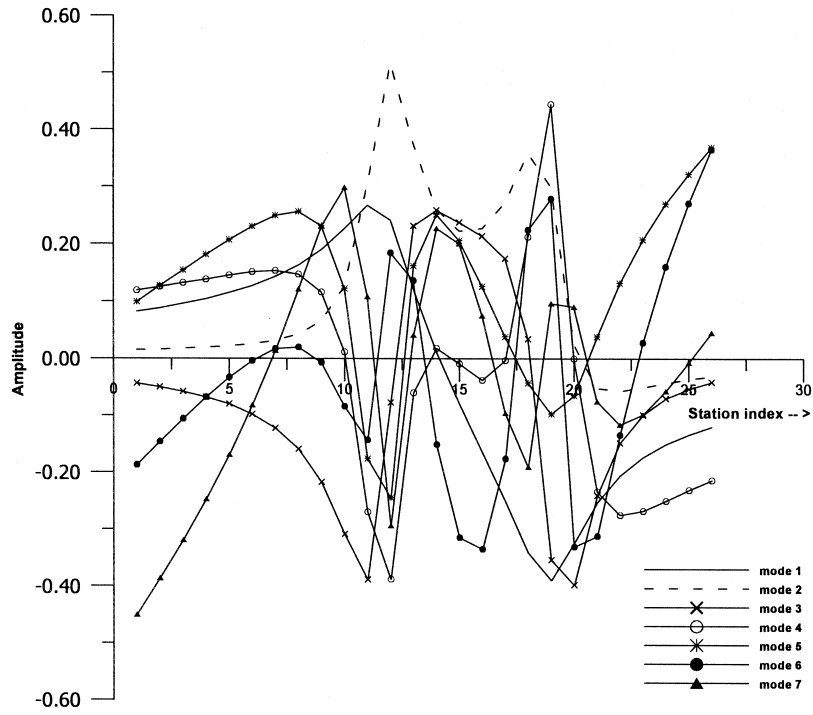


Fig. 4—Column vectors Up. station index vs modes(1-7) amplitude.

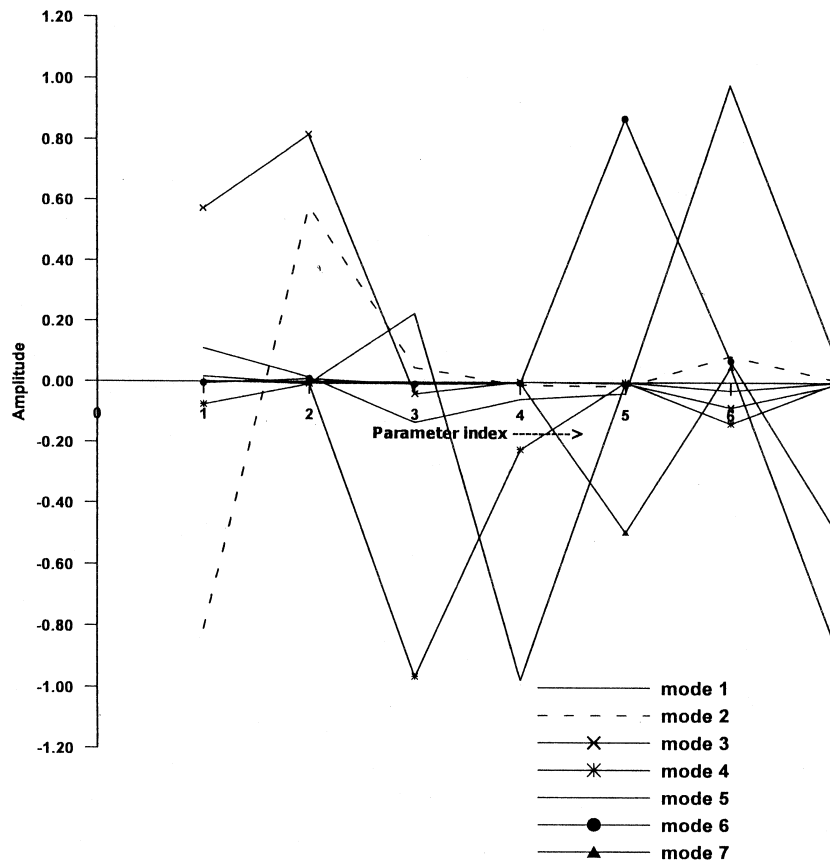


Fig. 5—Column vectors of Vp - Parameter index vs modes(1-7) amplitudes.

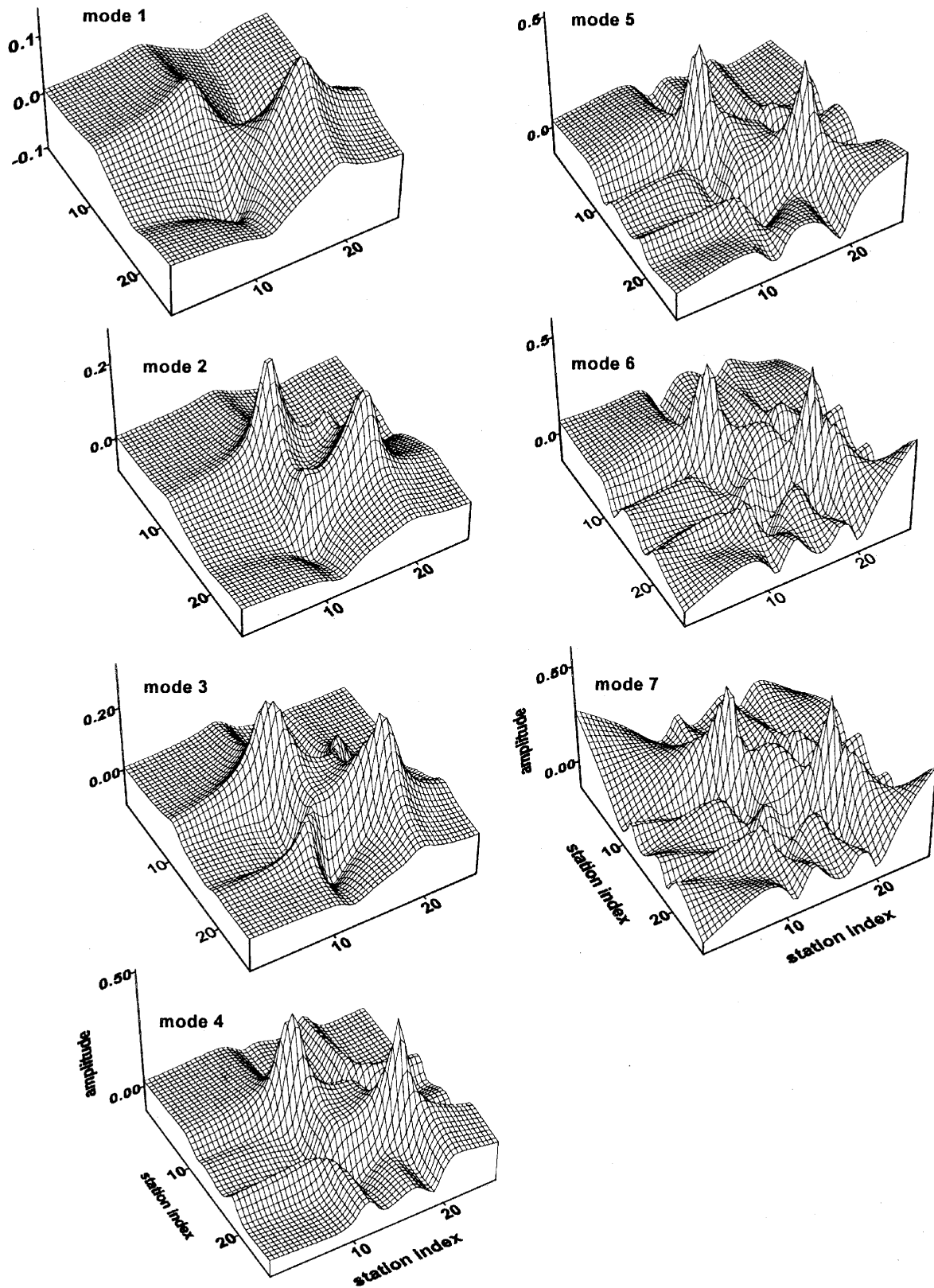


Fig. 6—3D-data resolution matrix modes (1 to 7).

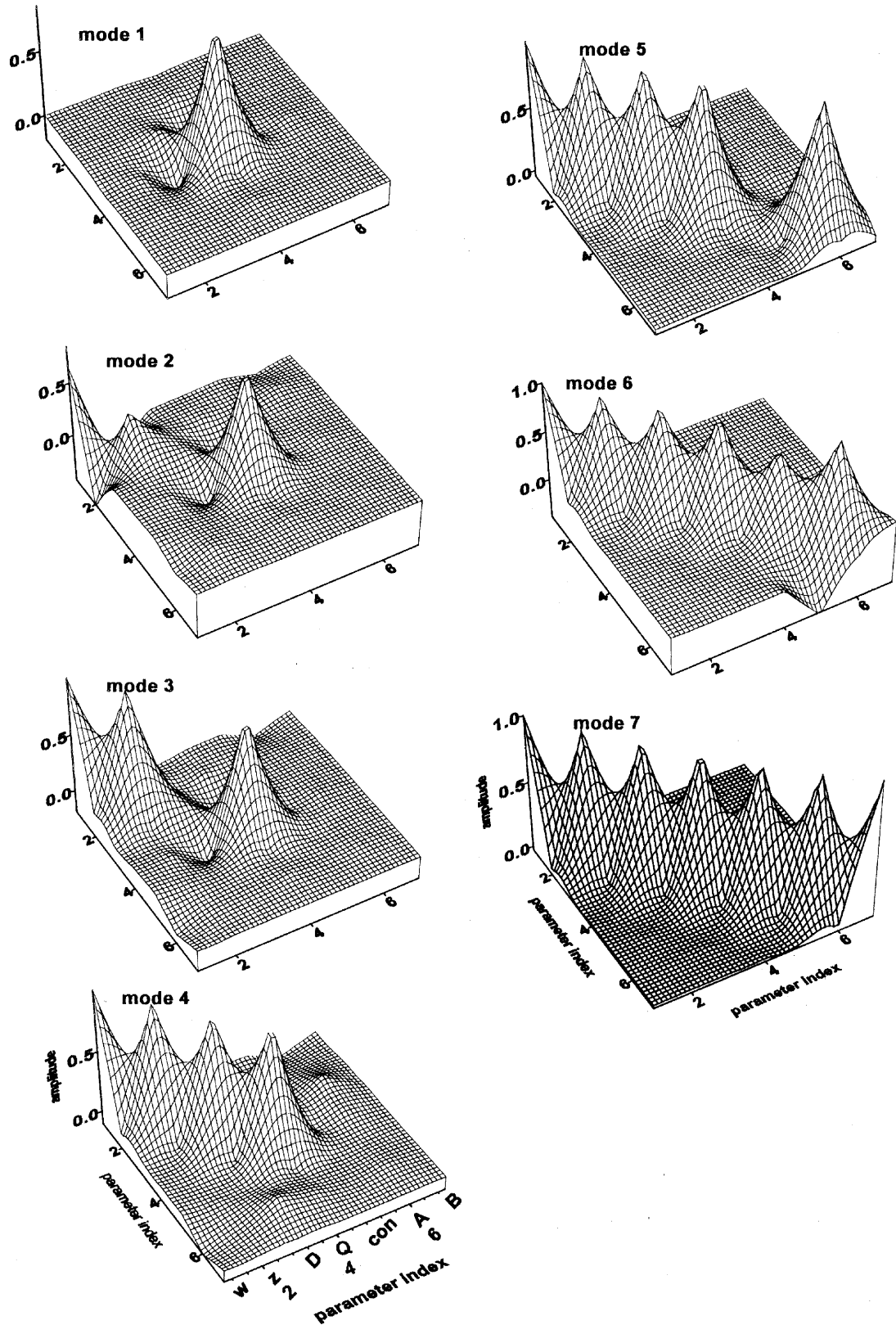


Fig. 7—3-D Model resolution matrix modes (1 to 7).

Table 2—Diagonal elements of model resolution ($V_p V_p^T$)

Model/Factor	w	z	D	Q	C	A	B
1	0.0003	0.0001	0.0513	0.9476	0.7807	0.0007	0.21E-6
2	0.6563	0.3340	0.0535	0.9477	0.0002	0.0083	0.00005
3	0.9824	0.9996	0.0550	0.9477	0.0002	0.0149	0.00009
4	0.9876	0.9996	0.9823	0.9968	0.0002	0.0331	0.00009
5	0.9999	0.9998	0.9999	0.9999	0.0015	0.9927	0.00590
6	1.0000	0.9999	0.9999	1.0000	0.7568	0.9976	0.24560
7	1.0000	1.0000	1.0000	1.0000	1.0000	1.0000	1.00000

Table 3—Diagonal elements of data resolution ($U_p U_p^T$) for each factor ($r = 1$ to 7)

Mode No	Station Index												
	0	1	2	3	4	5	6	7	8	9	10	11	12
1 mode	.007	.008	.009	.011	.013	.016	.020	.027	.027	.051	.071	.058	.015
2 modes	.007	.008	.009	.011	.014	.017	.021	.029	.041	.067	.164	.326	.068
3 modes	.009	.011	.013	.016	.020	.026	.036	.054	.054	.087	.162	.314	.332
4 modes	.023	0.26	0.30	.035	.041	.049	.060	.075	.101	.163	.387	.481	.213
5 modes	.033	.042	.054	.068	.084	.102	.122	.141	.154	.178	.418	.541	.239
6 modes	.068	.064	.065	.072	.085	.102	.122	.141	.154	.185	.438	.575	.257
7 modes	.270	.213	.167	.133	.113	.109	.122	.156	.208	.274	.450	.661	.259

Mode No	Station Index												
	13	14	15	16	17	18	19	20	21	22	23	24	25
1 mode	.000	.006	.027	.063	.116	.151	.104	.064	.042	.030	.023	.018	.014
2 modes	.056	.078	.136	.244	.240	.105	.660	.045	.033	.024	.019	.015	.015
3 modes	.219	.135	.112	.124	.167	.245	.365	.262	.124	.067	.042	.029	.017
4 modes	.135	.112	.125	.167	.290	.562	.262	.178	.143	.114	.092	.075	.062
5 modes	.198	.154	.141	.168	.292	.571	.266	.179	.160	.156	.164	.178	.198
6 modes	.221	.253	.252	.199	.342	.649	.375	.276	.178	.157	.189	.251	.330
7 modes	.272	.293	.258	.208	.378	.658	.383	.282	.191	.167	.192	.251	.331

Table 4—Percentage contribution of individual components of model space *s* (m)

Parameters	v ₁ %	v ₂ %	v ₃ %	v ₄ %	v ₅ %	v ₆ %	v ₇ %
W	.837	-9.693	4.972	-.427	.153	.000	.000
Z	-.186	6.917	7.106	-.046	.021	.001	.000
D	10.504	.562	-.340	-5.563	-.185	.000	.000
Q	-45.222	-.108	.009	-1.282	-.078	.000	.000
Const	.000	-.168	-.026	.000	-.050	.046	-0.19
A	-1.255	1.041	-.714	-.780	1.361	.004	.002
B	.000	.084	-.061	-.012	.107	-.026	-.033
Total (%)	58.003	18.573	13.228	8.111	1.454	0.0078	0.054

Table 5—Percentage contribution of individual component of data space *s*(d)

Station ID	u ₁ %	u ₂ %	u ₃ %	u ₄ %	u ₅ %	u ₆ %	u ₇ %
0	1.004	.079	-.138	.233	.042	-.003	-.006
1	1.121	.085	-.0157	.245	.054	-.003	-.005
2	1.223	.095	-.182	.258	.065	-.002	-.004
3	1.325	.106	-.213	.270	.077	-.001	-.003
4	1.465	.116	-.251	.284	.088	-.001	-.002
5	1.618	.137	-.307	.296	.098	.000	-.001
6	1.821	.169	-.383	.299	.106	.000	-.001
7	2.076	.227	-.499	.288	.109	.000	.002
8	2.420	.349	-.681	.227	.098	-.002	.003
9	2.891	.671	-.966	.023	.052	-.003	.004
10	3.401	1.612	-1.217	-.526	-.075	.003	.001
11	3.070	2.732	-.242	-.757	-.104	.003	-.004
12	1.554	1.981	.725	-.117	.068	-.003	.001
13	.153	1.379	.809	.036	.107	-.006	.003
14	-1.006	1.173	.743	-.018	.087	-.006	.003
15	-2.089	1.199	.668	-.074	.053	-.003	.001
16	-3.184	1.437	.546	-.006	.016	.004	-.001
17	-4.330	1.892	.107	.415	-.018	.005	-.002
18	-4.955	1.580	-1.107	.869	-.041	.005	.001
19	-4.114	.132	-1.245	.000	-.028	-.006	.001
20	-3.210	-.275	-.753	-.456	.016	-.006	-.001
21	-2.611	-.301	-.464	-.536	.056	-.002	-.002
22	-2.203	-.264	-.311	-.523	.088	.001	-.001
23	-1.911	-.227	-.220	-.487	.114	.003	-.001
24	-1.694	-.190	-.166	-.450	.136	.005	.000
25	-1.516	-.164	-.129	-.417	.156	.007	.001
Total	58.003	18.573	13.228	8.111	1.954	.078	.054

58% of total distribution representing model parameters *Q* followed by *D*, *w*, and *z* in that order. In general, *Q* - an angle, function of θ , ϕ , D_m , i and α , contributes to the extent of 45% between stations 18 and 21. Further $z < w$, indicating that it is thick dyke intrusive. The contribution of remaining three functions in *s*(d) and *s*(m) is only 2% of total information, and is too insignificant to consider for interpretation.

Therefore the first four energetic spatial and model functions of *s*(d) and *s*(m) have been used to bring the predictable rich part of the original signal to obtain inverse solution (Fig. 3B) by operating GI on magnetic anomaly and for construction of data and model resolution matrices in 3-D form (Figs. 6 and 7). At the end of 21 iterations the results obtained from GI indicate that the width of the dyke intrusive model is 0.72 km at a depth (*Z*) of 0.12 km from the surface

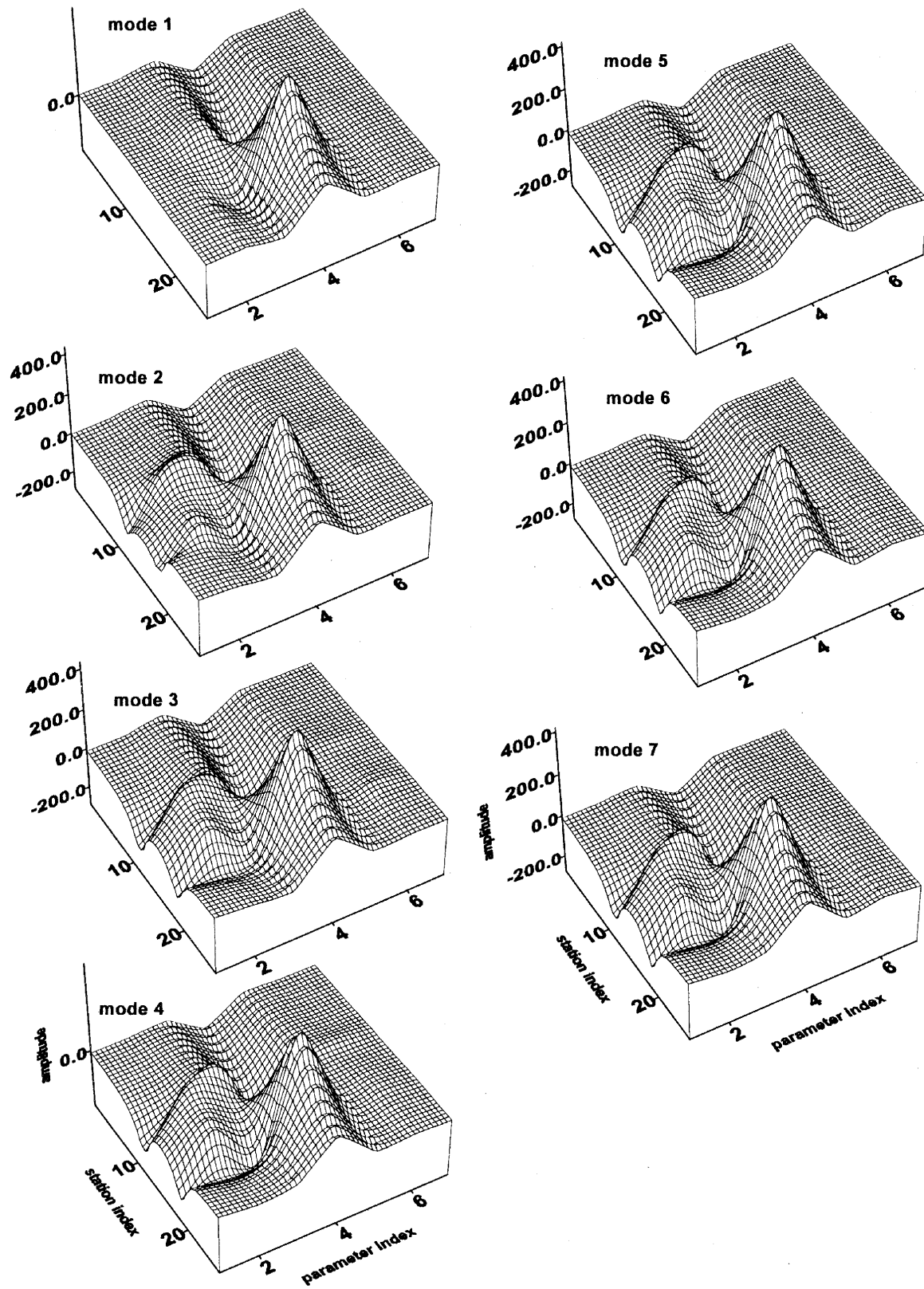


Fig. 8—3D-filtered data kernel matrix (mode 1 to 7).

located at (D) 1.44 km away from the reference point and at an angle (Q) of 140° and with intensity of magnetization (C) 225.86 nT (Fig 3B). The optimized value of intensity of magnetization (C) is reasonably comparable with local value (250. nT) ¹². Computed model anomaly with refined parameter set almost coincides with observed field anomaly to quantify (Fig. 3B). The initial objective function (=111039) is reduced up to (=4645) after 21 iterations, and the corresponding refined model parameter set is considered for interpretation. The refined intrusive dyke model corresponding to minimum objective function is shown in Fig.3B. The Root Mean Square (RMS) error for the field data at zero iteration is 65.35. After 21 iterations it has reduced to 13.36.

Data resolution

The data resolution matrix is an indication of the information density of the data kernel i.e. it indicates which data contribute independent information to the solution. The diagonal elements of $U_p U_p^T$ are shown in Table 3 for factors 1 to 7. A value of unity indicates contribution of information independent of other observations. From Table 3 one can infer which of the data points contribute strong/poor information resolution. The data resolution is given by $N = MM^T_g = U_p U_p^T$. The data are completely resolved if U_p spans the complete space of data. The small eigenvalues in the data kernel increases the rank of the matrix (i.e. the dimension of activated space) besides amplifying the solution due to the presence of noise. Such a filtered data kernel has been utilized in 3-D form (Fig. 8), which almost represents the original data kernel to build GIO. In Fig. 6 Factor 1 describes the contour map of data resolution matrix $u_1 u_1^T$, where u_1 is the highest spatial energetic mode of $s(d)$. It gives 58.003% variance of the total information i.e. mostly gross features of the kernel (Table 5). High resolution was found at stations 10 and 18 indicating the sudden change at these stations likely indicating the width of the dyke intrusive (Fig. 6 and Tables 3-5).

Model resolution

The model resolution of the generalised inverse is given by $R = M^T_g M = V_p V_p^T$. Here p indicates number of factors used in SVD, which is less than or equal to the rank of the matrix M . The model parameters will be perfectly resolved if V_p spans the complete space of the model parameters i.e. $V_p V_p^T = I_m$. The model resolution is perfect for the contribution of magnetic anomaly due to Q (Fig. 7, factor 1 and

shown in Table 4) and one can conclude that Q is independent of other model parameters and of homogeneous nature which is also reflected in the data resolution Fig. 6, factor 1 at stations 12 and 18 (also see Table 5). Table 4 presents the individual parameter contribution in each of the seven factors. In first factor the contribution of Q is 45.222% out of 58%, and in second factor the contribution of W is 9.7% out of 18.5%, and in third factor z contributes 7.1% out of 13.2% and finally in fourth factor that of D is 5.5% out of 8.1%. The total contribution of Q , w , z and D is 62% out of 89.8% from the first four factors.

From the above model and data resolution study, the partial information contained in the data space is adequate enough to reconstruct the approximate model parameters. This reveals the efficacy of natural generalised inverse GI with a least square sense in handling problems of over determinacy.

Acknowledgement

The authors are thankful to Director, National Institute of Oceanography, Goa, for his encouragement.

References

- 1 Malleswara Rao M M, Narayana S L, Subrahmanyam A S & Murthy K S R, Two computer programs for the analysis of marine magnetic data, *Comp & Geosci*, 19 (1993) 657-672.
- 2 Sarma K V L N S, Ramana M V, Murty G P S, Subrahmanyam V, Krishna K S, Chaubey A K, Malleswara Rao M M & Narayana S L, Application of Inversion techniques on marine magnetic data-Andaman shelf, *J. Geol. Soc. India*, 44(1994) 73-78
- 3 Tarantola A, *Inverse problem theory: methods for data fitting and model parameter estimation* (Elsevier, Amsterdam) 1987, pp.613.
- 4 Backus G E & Gilbert J F, Numerical application of formalism for geophysical inverse problems, *Geophys. J. Roy. Astr. Soc.*, 13(1968) 247-276.
- 5 Murthy K S R, Malleswara Rao M M, Rao T C S & Subrahmanyam A S, A comparative study of Werner Deconvolution and conventional modelling of marine magnetic data, *Geophys. Res. Bull.*, 25 (1987) 152-157.
- 6 Murthy, K S R, Rao T C S, Subrahmanyam A S, Malleswara Rao M M & Narayana S L, Structural lineaments from the magnetic anomaly maps of the eastern continental margin of India (ECMI) and NW Bengal Fan, *Mar. Geol.*, 114 (1993) 171-183.
- 7 Menke W, *Geophysical data analysis: discrete inverse theory*, (Academic Press, New York) 1984, pp.260.
- 8 Ramana Murty T V, Veerayya M & Murty C S, Sediment size distributions of the beach and near shore environs along the central west coast of India: analysis using EOF, *J. Geophys. Res.*, 91(1986) 8523 -8526.
- 9 Marquardt D W, An algorithm for least-squares estimation of non-linear parameters, *J. Soc. Indust. Appl. Math.*, 11 (1963) 431-441.

- 10 Pedersen L B, Interpretation of potential field data—A generalised inverse approach, *Geophy. Prosp.* 25 (1977) 199-230.
- 11 Radhakrishna Murthy I V, Swamy K V & Jagannadha Rao S, Automatic inversion of magnetic anomalies of faults, *Comp & Geosci*, 27 (2001), 315 -325.
- 12 Radhakrishna Murthy I V & Rama Rao P, Magnetic anomalies and basement structure around Vijayanagaram, Visakhapatnam and Srikakulam Districts of Andhra Pradesh, India, *Gond. Res.*, 4(2001) 443-454.
- 13 Radhakrishna Murthy I V, *Gravity and magnetic interpretation in exploration geophysics*, Memoir 40 (Geological Society of India, Bangalore) 1998, pp. 363.
- 14 Radhakrishna Murthy I V, Magnetic anomalies of two-dimensional bodies and algorithms for magnetic inversion of dykes and basement topographies, *Proc. Indian Acad. Sci. (Earth & planet. Sci.)*, 99(1990) 549-579.
- 15 Malleswara Rao M M, Ramana Murty T V, Murthy K S R & Vasudeva R Y, Application of natural generalised inverse technique in reconstruction of gravity anomalies due to a fault, *Indian J. Pure. Appl. Math.*, 34 (2003) 31-47.
- 16 Ramana Murty T V, Somayajulu Y K & Murty C S, Reconstruction of sound speed profile through natural generalised inverse technique, *Indian J. Mar. Sci.*, 25(1996) 328-334.
- 17 Ramana Murty T V, Somayajulu Y K, Mahadevan R, Murty C S & Sastry J S, A solution to the inverse problem in ocean acoustics, *Defence Sci J*, 42 (1992) 89-101.
- 18 Jackson D D, Interpretation of inaccurate, insufficient and inconsistent data, *Geophys J.R. Astr. Soc.*, 28 (1972) 97-109.
- 19 DGRF IAGA, Division 1, working group, International Geomagnetic Reference Field, *EOS*, 67(1986) 523-524.

Notation

J	-	intensity of effective magnetization of two-dimensional body lying in a plane perpendicular to the strike
ϕ	-	dip of the effective magnetization
α	-	strike of the body measured from the magnetic north due east or west
i	-	dip of the earth's magnetic field
F	-	Earth's magnetic field expressed in gammas
D_m	-	direction of measurement, is 0 for horizontal ΔH , $\Pi/2$ for vertical ΔV and i for the total field ΔF anomalies
ΔT	-	anomaly in any component : it is equal to ΔH , ΔV and ΔF when D_m is 0, $\Pi/2$ and i respectively.
ΔT_{cal}	-	calculated anomaly
dT	-	$(\Delta T_{obs} - \Delta T_{cal})$
K	-	susceptibility contrast of the body
θ	-	geological dip of the dyke model
Q	-	an angle, which is a function of θ , ϕ , D_m , i and α
D	-	distance from an arbitrary reference point to the position of centre of the dyke
x	-	distance co-ordinates of anomalies
w	-	half width of the dyke
C	-	size factor, being a function of magnetisation (in gammas) and dip of dyke
z	-	depth to the top of the dyke
N_{OBS}	-	Number observations
A'	-	regional gradient
B'	-	regional at the first station